Optical Diffraction Radiation of a Beam of Particles Flowing Near a Circular Silver Nanowire

Dariia O. Yevtushenko[1,2]

[1]Department of Photonics and Laser Engineering, Kharkiv National University of Radio Electronics, Kharkiv 61066, Ukraine
[2]Laboratory of Micro and Nano Optics, Institute of Radio-Physics and Electronics NASU, Kharkiv 61085, Ukraine

dariia.yevtushenko@gmail.com

Abstract—**The optical diffraction radiation that accompanies the motion of a modulated beam of electrons near a silver nanowire scatterer is investigated in the two-dimensional formulation. Our goal is to compute the field in the near and far zones and analyze how it depends on electron beam parameters. We demonstrate the excitation of plasmon resonances of such a nanoscale scatterer that can be used in the design of optical range non-invasive beam position monitors.**

Index Terms— **diffraction radiation, nanowire scatterers, plasmon resonance, surface wave, total scattering cross-section, absorption cross-section**

I. Introduction

Since long ago, it was known that charged particles, such as electrons, radiate electromagnetic waves when moving through the boundary between material media – this is called the transition radiation. The radiation of electrons moving in vacuum without crossing any material boundaries attracted the attention of researchers much later. The most known example of such effect is the Smith-Purcell radiation [1-13]; it is associated with an electron beam flowing over a periodic grating, for instance, ruled on a metal surface. Still the Smith-Purcell radiation is only a particular case of more general phenomenon: the radiation of the surface and polarization currents induced on the metal and dielectric objects by the electron beams flowing in their vicinity however without touching them. This type of electromagnetic-wave radiation is commonly called the *diffraction radiation* (DR) [3-13]. As known, the characteristics of beam monitors can be enhanced if the scatterers are shaped as cavities, thanks to the associated high-Q resonances [3].

Today DR is considered as the most promising technique for noninvasive beam monitoring and diagnostics [6-10] in charged-particle accelerators. This is because the directional shape of the far-field pattern and the amount of DR power values depend on the electron-beam parameters such as bunching, velocity, and distance between the beam and the scatterer.

Detection of DR in the visible wavelength region, called the optical DR, is of the special interest because rapid development of nanotechnologies opens the way to use micro and nanoscale scatterers. Such scatterers can be also designed to display the resonances from ultraviolet to infrared wavelengths. The associated resonances are then either on the low-order modes of dielectric objects or the localized surface plasmon (LSP) modes of noble-metal objects [14-16]. Note that the plasmonic scatterers can be designed tunable if covered with the graphene [17-20]. Nanoscale dimensions of such beam-sensor antenna elements help reduce distortion to the electron beam velocity and power, which therefore can be assumed fixed. Under such assumption, called *fixed-current approximation*, one can perform engineering analysis of the beam monitors like it is done in the traditional antenna theory: DR can be treated as the wave scattering phenomenon. In this work, we apply the outlined approach to study the optical DR in the presence of a circular silver nanowire as a simplest nanocavity.

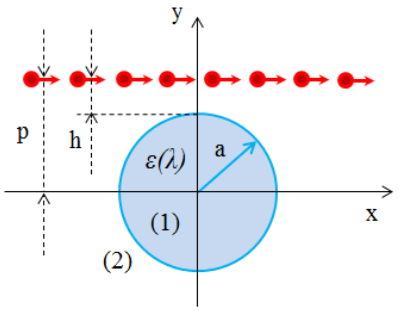

Fig. 1. Modulated electron beam flowing near a circular silver nanowire.

II. Scattering Configuration and Beam Field

Consider a zero-thickness two-dimensional (2-D) beam of charged particles, which flows along the straight trajectory with velocity $v = \beta c$ ($\beta < 1$) at the distance h from a circular silver nanowire. The wire radius is a and its dielectric permittivity ε depends on the wavelength. Denote the inner and the outer domains of the wire as domains (1) and (2), respectively, and introduce the Cartesian and the polar coordinates as shown in Fig. 1. Hence, the beam distance from the x-axis is $p = h + a$.

Assume that the particle density is modulated with the cyclic frequency ω. Then the charge density function has a harmonic time dependence $e^{-i\omega t}$ and is given by

$$\rho = \rho_0 \delta(y - p) \exp[i(kx/\beta - \omega t)], \qquad (1)$$

where $\delta(\cdot)$ is the Dirac delta function, ρ_0 is the amplitude of the beam modulation, and $k = \omega / c$ is the free-space wavenumber (c is the light velocity). The modulation of the

electron beam can be achieved by its preliminary bunching in a periodic waveguide or directly by a laser emission [7,13].

According to [2], the Coulomb field of the beam (1) is a inhomogeneous plane wave, the single component of the magnetic field of which is given by the expression

$$H_z^{in}(x,y) = A\,\mathrm{sign}(y-p)e^{-q|y-p|}e^{i(k/\beta)x}, \qquad (2)$$

where $q = k\gamma/\beta$, $\gamma = (1-\beta^2)^{1/2}$, function sign(•) is the sign of the argument, the time dependence is omitted, and $A>0$ is a constant. This is a slow surface wave running in the positive direction of the *x*-axis. Note that the function (2) has a jump at the trajectory $y = p$ that corresponds to the electric current.

Our aim is to determine the total electromagnetic field of beam (1) in the presence of the wire. We will consider the associated scattering problem assuming that the beam velocity β is a constant, i.e. in the given-current approximation.

III. Formulation of the Wave Scattering Problem

The surface currents, induced on the wire by the incident field (2), generate the scattered field $H_z^{(2)}$ and modify the field in the inner domain, $H_z^{(1)}$. Then the total field in the outer domain can be presented as $H_z^{tot} = H_z^{in} + H_z^{(2)}$. The unknown functions must satisfy the following conditions:

1. The Helmholtz equation with coefficient $k_1 = \alpha k$ in domain (1) and $k_2 = k = \omega/c$ in domain (2),

$$(\Delta + k_{1,2}^2)H_z^{(1,2)}(\vec{r}) = 0 \qquad (3)$$

2. The boundary conditions at $r = a$ and $0 \le \varphi < 2\pi$,

$$H_z^{(1)} = H_z^{in} + H_z^{(2)}, \quad E_\varphi^{(1)} = E_\varphi^{in} + E_\varphi^{(2)}, \qquad (4)$$

where the electric field φ-component relates to the magnetic field as $E_\varphi^{(1,2)} = Z_0(ik\varepsilon_{1,2})^{-1}\partial H_z^{(1,2)}/\partial r$, $Z_0 = (\mu_0/\varepsilon_0)^{1/2}$ is the free-space impedance, and $x = r\sin\varphi$, $y = r\cos\varphi$.

3. The condition of the local power finiteness.

4. The radiation condition at infinity (outgoing wave behavior),

$$H_z^{(2)}(r,\varphi) \sim 2^{1/2}(i\pi k_2 r)^{-1/2}e^{ik_2 r}\Phi(\varphi) \text{ at } r\to\infty, \qquad (5)$$

As known, the conditions 1 to 4 guarantee the solution uniqueness.

IV. Basic Equations

The circular shape of the wire boundary suggests the use of the method of separation of variables, in the polar coordinates. Therefore we expand the field functions in each domain in terms of Fourier series in the angular coordinate φ, in particular, if $y = r\sin\varphi < p$ then

$$H_z^{in}(\vec{r}) = -Ae^{-qp}e^{ikr\cos(\varphi+\psi)}, \qquad (6)$$

where we introduce the complex incidence angle ψ, such that

$$\cos\psi = 1/\beta, \quad \sin\psi = i\gamma/\beta. \qquad (7)$$

The function (6) has the known representation as a Fourier series,

$$H_z^{in}(\vec{r}) = -Ae^{-q(h+a)}\sum_{m=-\infty}^{+\infty} i^m J_m(kr)(1-\gamma)^m\beta^{-m}e^{im\varphi} \qquad (8)$$

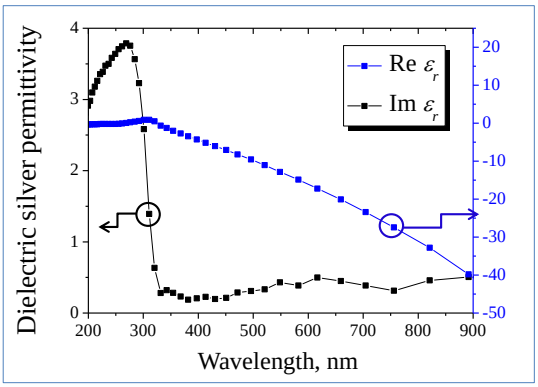

Fig. 2. Bulk complex relative permittivity function of silver versus the wavelength.

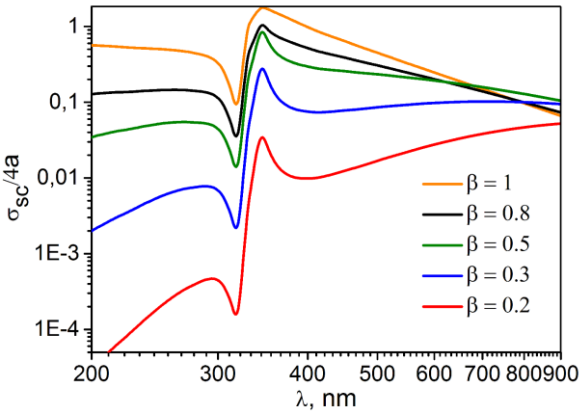

Fig. 3. Normalized TSCS of the 50-nm radius silver nanowire versus the wavelength in the visible range, for several values of the electrons' relative velocity β.

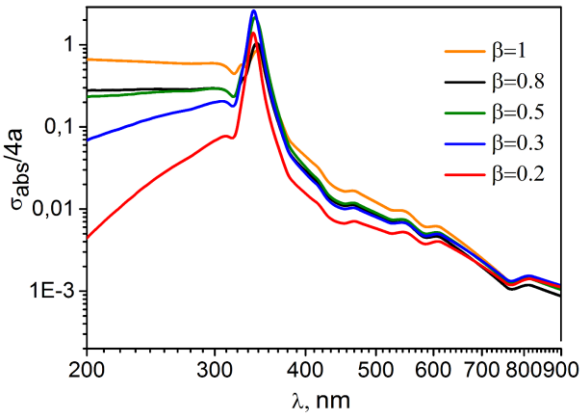

Fig. 4. Normalized ACS of the same nanowire versus the wavelength.

Then the scattered field is presented as

$$H_z^{sc}(\vec{r}) = \begin{Bmatrix} H_z^{(1)}, & r<a \\ H_z^{(2)}, & r>a \end{Bmatrix} = \sum_{m=-\infty}^{+\infty} \begin{Bmatrix} a_m J_m(k_1 r), & r<a \\ b_m H_m^{(1)}(kr), & r>a \end{Bmatrix} e^{im\varphi}, \qquad (9)$$

where a_m, b_m are unknown coefficients and J_m and $H_m^{(1)}$ are the Bessel and the first-kind Hankel functions. The coefficients are found using the conditions 1. to 4. in analytical form as

$$a_m = C\left[f_m(ka)H'_m(ka) - H_m(ka)f'_m(ka)\right](\Delta_m)^{-1}, \qquad (10)$$

$$b_m = C\left[f_m(ka)\alpha J'_m(k\alpha a) - J_m(k\alpha a)f'_m(ka)\right](\Delta_m)^{-1}, \qquad (11)$$

where the superscripts of the Hankel functions and their derivatives are omitted, and other notations are

$$C = -Ae^{-q(h+a)}, \tag{12}$$

$$f_m = i^m J_m(ka)(1-\gamma)^m \beta^{-m}, \quad f'_m = i^m J'_m(ka)(1-\gamma)^m \beta^{-m}, \tag{13}$$

$$\Delta_m = J_m(k\alpha a)H'_m(ka) - \alpha J'_m(k\alpha a)H_m(ka), \tag{14}$$

Here, characteristic equations of the considered scatterer,

$$\Delta_m(\lambda) = 0, \quad m = 0, \pm 1, \pm 2, \ldots, \tag{15}$$

may have only complex solutions, λ_{mn}, which form a discrete set with non-zero imaginary parts. These are complex natural wavelengths of the modes of a circular wire as open cavity.

We characterize the scatterer with its total scattering cross-sections (TSCS) (17) and absorption cross-sections (ACS). TSCS is the result of integration of the Poynting vector flux of the scattered field over all space directions,

$$\sigma_{sc} = \frac{4}{kA^2} \sum_{m=-\infty}^{+\infty} |b_m|^2, \tag{16}$$

ACS is obtained with the aid of the Optical Theorem (a.k.a Complex Poynting Theorem) applied to the total field function and its complex conjugate. With account of (7), it takes form of

$$\sigma_{abs} = -\frac{4}{kA^2} e^{-qp} \operatorname{Re} \sum_{m=-\infty}^{+\infty} i^m b_m \left(\frac{1-\gamma}{\beta}\right)^m - \sigma_{sc} \tag{17}$$

Presented further results for (16) and (17) are normalized by $4a$ that is the limit value of σ_{sc} at $\beta = 1$ and $a/\lambda \to \infty$.

V. Numerical Results

We have studied the DR characteristics for the scatterer shaped as a circular dielectric wire shown in Fig. 1. The complex-valued bulk dielectric permittivity of silver has been taken from the paper of Johnson and Christy [21] and combined with a cubic spline interpolation (Fig. 2). In computations, the associated series have been truncated at the number ±10 that well exceeds the maximum of the values ka and $ka|\alpha|$ in the whole optical range and provides 6 and more correct digits.

The plots in Fig. 3 demonstrate the dependences of the normalized TSCS on the modulation wavelength in the visible range, for the wire with the radius 50 nm, the separation distance h = 10 nm, and several values of the relative beam velocity β. For all β, the plots of TSCS show the maximum at λ = 347 nm, preceded by the minimum at λ = 318 nm.

The graphs in Fig. 4 demonstrate the modulation wavelength dependences of the normalized ACS for the same silver nanowire. They show essentially only the maximum at λ = 343 nm. Note that ACS is quite comparable with TSCS, especially in the blue and violet parts of spectrum.

As expected, the wavelengths of the peak scattering and peak absorption are very close to the root of the "textbook" quasi-static equation, $\operatorname{Re}\varepsilon(\lambda) = -1$ [14,15], found at λ = 338 nm [21]. This is a collective resonance caused by the infinite number (m = 1,2,…) of the transverse LSP modes of a circular wire with negative dielectric function, because if $a/\lambda \to 0$, then $\Delta_m(\lambda) \approx \varepsilon(\lambda) + 1 + O(m^{-1}a^2\lambda^{-2})$ [15]. The separate LSP resonances merge together because of the losses in silver.

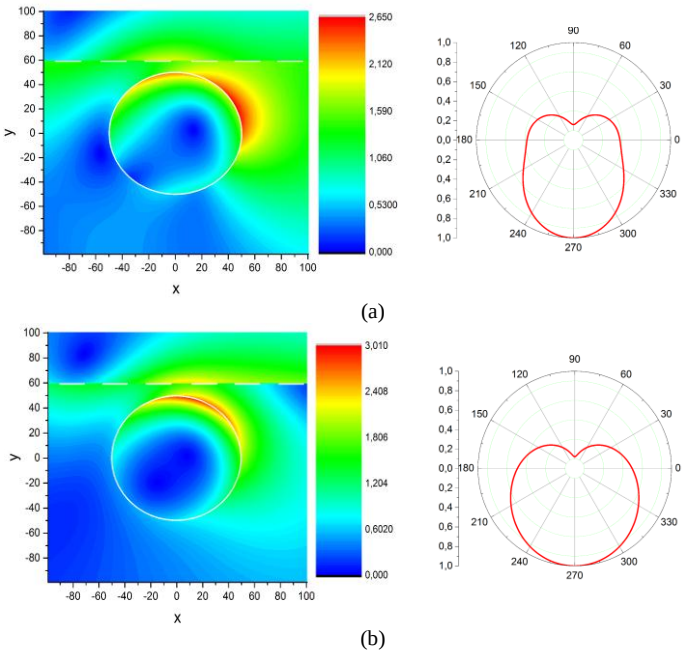

(a)

(b)

Fig. 5. Near magnetic field patterns (left) and normalized far-field scattering pattern (right) of the silver nanowire of the radius a = 50 nm for λ = 347 nm and β = 0.8 (a), β = 0.5 (b) in the LSP resonance.

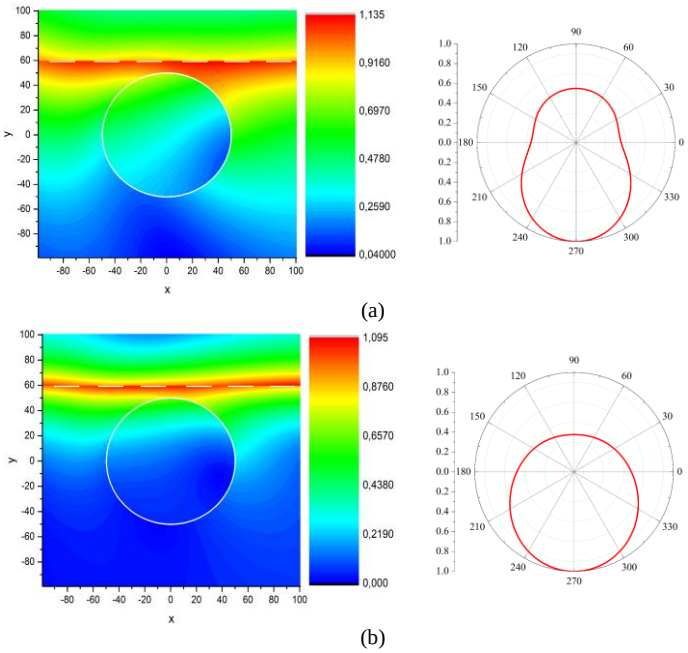

(a)

(b)

Fig. 6. The same as in Fig. 4 however for the λ = 318 nm in the minimum of TSCS plots.

The minimum of TSCS (and to lesser extent of ACS) is typical for the plasmonic scatterers, see [17-20]. Its location in wavelength corresponds to the value, at which the dielectric function of silver comes near to 1, $\operatorname{Re}\varepsilon(\lambda) = 1$. Here the metal becomes optically transparent although still not invisible due to small absorption. According to [21], that happens at λ = 308 nm, and the red shift is the effect of finite wire radius. As can be found after inspection of the works [22-25], this

"invisibility" effect is equally well observable in the scattering of light by finite and infinite arrays of circular silver nanowires. Potentially such optical transparency can be also useful in the design of beam velocity sensors.

We have computed the near magnetic field patterns and the normalized far-field angular scattering patterns of the same silver nanowire, at the fixed values of β and λ. As one can see in Fig. 5, at the resonance wavelength the field bright spots are located near the surface of the nanowire and do not penetrate into it. This is explained by the surface nature of the plasmon modes.

At the "invisibility wavelength," the total field in the near zone shows the beam field (2) only slightly perturbed by the wire – see Fig. 6.

The shape of the far-field DR patterns can be explained by the contribution of the field part, which is anti-symmetric with respect to the wire center (along the *y*-axis). Its maximum is always oriented in the normal direction to the beam trajectory.

VI. Conclusions

We have studied, in the fixed-current approximation, the optical diffraction radiation that accompanies the motion of the charged-particle beam near a plasmonic silver nanowire. As we have shown, the radiated power is enhanced near the natural-mode wavelength of the plasmonic nanowire open resonator. This can be used in the design of nanoscale beam position sensors and monitors. Unlike the diffraction radiation in the presence of dielectric nanowire, the metal nanowire also displays the effect of "invisibility" at the wavelength close to the optical transparency of metal. It can be noted that in-resonance fields are shaped as rotating surface waves made of two degenerate LSP modes with nearly $\pi/2$ phase shift. This happens because, unlike the plane-wave field, the beam field depends on *y*, and hence can excite each of two degenerate (symmetric and the anti-symmetric) natural LSP modes of the wire.

References

[1] S. J. Smith and E. M. Purcell, "Visible light from localized surface charges moving across a grating," *Phys. Rev.*, vol. 92, art. 1069, 1953.

[2] P. M. van den Berg, "Smith-Purcell radiation from a line charge moving parallel to a reflection grating," *J. Opt. Soc. Am.*, vol. 63, no 6, pp. 689-698, 1973.

[3] A. I. Nosich, "Diffraction radiation which accompanies the motion of charged particles near an open resonator," *Radiophysics Quant. Electron.*, vol. 24, no 8, pp. 696-701, 1981.

[4] E. I. Veliev, A. I. Nosich, and V. P. Shestopalov, "Radiation of an electron flux moving over a grating consisting of cylinders with longitudinal slits," *Radiophysics Quant. Electron.*, vol. 20, no 3, pp. 306-313, 1977.

[5] M. Castellano, "A new non-intercepting beam size diagnostics using diffraction radiation from a slit," vol. 394, pp. 275-280, 1997.

[6] A. P. Potylitsyn, "Resonant diffraction radiation and Smith-Purcell effect," *Phys. Lett. A*, vol. 238, pp. 112-116, 1998.

[7] M. Castellano, *et al*., "Measurements of coherent diffraction radiation and its application for bunch length diagnostics in particle accelerators," *Phys. Rev. E*, vol. 63, art. no 056501, 2001.

[8] P. Karataev, S. Araki, R. Hamatsu, *et al*., "Beam-size measurement with optical diffraction radiation at KEK accelerator test facility," *Phys. Rev. Lett*., vol. 93, art. no 244802, 2004.

[9] Y. A. Goponov, R. A. Shatokhin, and K. Sumitani, "Diffracted diffraction radiation and its application to beam diagnostics," *Nuclear Instrum. Meth. A*, vol. 885, pp. 134–138, 2018.

[10] L. Bobb, R. Kieffer, *et al*., "Feasibility of diffraction radiation for noninvasive beam diagnostics as characterized in a storage ring," *Phys. Rev. Accel. Beams*, vol. 21, art. no 03801, 2018.

[11] T. Muto, S. Araki, *et al.*, "Observation of incoherent diffraction radiation from a single-edge target in the visible-light region," *Phys. Rev. Lett*.., vol. 90, no 10, pp. 104801-104804, 2003.

[12] N. Talebi, "Interaction of electron beams with optical nanostructures and metamaterials: from coherent photon sources towards shaping the wave function," *J. Opt*., vol. 19, art. no 103001, 2017.

[13] K. J. Leedle, A. Ceballos, H. Deng, et al., "Dielectric laser acceleration of sub-100 keV electrons with silicon dual-pillar grating structures," *Opt. Lett*., vol. 40, no, 18. pp. 4344-4347, 2015.

[14] C. F. Bohren and D. R. Huffman, *Absorption and Scattering of Light by Small Particles*, Wiley-VCN Publ, Weinheim, 2004.

[15] E. A. Velichko and D. M. Natarov, "Localized versus delocalized surface plasmons: dual nature of resonances on a silver circular wire and a silver tube of large diameter," *J. Optics*, vol. 20, no 7, art. no 075002/9, 2018.

[16] D. O. Yevtushenko, S. V. Dukhopelnikov, E. N. Odarenko, and A. I. Nosich, "Optical diffraction radiation of electron beam in the presence of a dielectric nanowire resonator," *Proc. Int. Conf. Mathematical Methods in Electromagn. Theory (MMET-2018)*, Kyiv, 2018, pp. 148-151.

[17] M. Riso, M. Cuevas and R. A. Depine, "Tunable plasmonic enhancement of light scattering and absorption in graphene-coated subwavelength wires," *J. Opt*., vol. 17, pp. 075001/8, 2015.

[18] M. Cuevas, *et al.*, "Complex frequencies and field distributions of localized surface plasmon modes in graphene-coated subwavelength wires," *J. Quant. Spect. Rad. Transfer*, vol. 173, pp. 26-33, 2016.

[19] M. Naserpour, C. J. Zapata-Rodríguez, S. M. Vuković, *et al.*, "Tunable invisibility cloaking by using isolated graphene-coated nanowires and dimers," *Sci. Rep.*, vol. 12, pp. 12186/14, 2017.

[20] V. I. Fesenko, V. I. Shcherbinin, and V. R. Tuz, "Multiple invisibility regions induced by symmetry breaking in a trimer of subwavelength graphene-coated nanowires," arXiv:1806.02529v1[physics.optics] 2018.

[21] P. B. Johnson and R. W. Christy, "Optical constants of the noble metals," *Phys. Rev. B*., vol. 6, no 12, pp. 4370-4378, 1972.

[22] D.M. Natarov, V.O. Byelobrov, R. Sauleau, T.M. Benson, A.I. Nosich, "Periodicity-induced effects in the scattering and absorption of light by infinite and finite gratings of circular silver nanowires," *Opt. Express*, vol. 19, no 22, pp. 22176-22190, 2011.

[23] V.O. Byelobrov, T.M. Benson, A.I. Nosich, "Binary grating of sub-wavelength silver and quantum wires as a photonic-plasmonic lasing platform with nanoscale elements," *IEEE J. Sel. Top. Quant. Electron.*, vol. 18, no 6, pp. 1839-1846, 2012.

[24] D. M. Natarov, R. Sauleau, M. Marciniak, and A. I. Nosich, "Effect of periodicity in the resonant scattering of light by finite sparse configurations of many silver nanowires," *Plasmonics*, vol. 9, no 2, pp. 389-407, 2014.

[25] D. M. Natarov, M. Marciniak, R. Sauleau, and A.I. Nosich, "Seeing the order in a mess: optical signature of periodicity in a cloud of plasmonic nanowires," *Opt. Express.*, vol. 22, no 23, pp. 28190–28198, 2014.